ELSEVIER

Biophysical Chemistry 104 (2003) 623–632

Biophysical Chemistry

www.elsevier.com/locate/bpc

Direct voltammetry and electrocatalytic properties of catalase incorporated in polyacrylamide hydrogel films

Haiyun Lu, Zhen Li, Naifei Hu*

Department of Chemistry, Beijing Normal University, Beijing 100875, PR China

Received 20 February 2003; received in revised form 20 February 2003; accepted 4 April 2003

Abstract

The direct voltammetry and electrocatalytic properties of catalase (Cat) in polyacrylamide (PAM) hydrogel films cast on pyrolytic graphite (PG) electrodes were investigated. Cat-PAM film electrodes showed a pair of well-defined and nearly reversible cyclic voltammetry peaks for Cat Fe(III)/Fe(II) redox couples at approximately −0.46 V vs. SCE in pH 7.0 buffers. The electron transfer between catalase and PG electrodes was greatly facilitated in the microenvironment of PAM films. The apparent heterogeneous electron transfer rate constant (k_s) and formal potential ($E^{\circ\prime}$) were estimated by fitting square wave voltammograms with non-linear regression analysis. The formal potential of Cat Fe(III)/Fe(II) couples in PAM films had a linear relationship with pH between pH 4.0 and 9.0 with a slope of −56 mV pH^{-1}, suggesting that one proton is coupled with single-electron transfer for each heme group of catalase in the electrode reaction. UV–Vis absorption spectroscopy demonstrated that catalase retained a near native conformation in PAM films at medium pH. The embedded catalase in PAM films showed the electrocatalytic activity toward dioxygen and hydrogen peroxide. Possible mechanism of catalytic reduction of H_2O_2 at Cat-PAM film electrodes was proposed.

Keywords: Catalase; Polyacrylamide; Film modified electrode; Direct electrochemistry; Electrocatalysis

1. Introduction

Study of direct electrochemistry of redox enzymes can provide a model for the mechanistic study of electron transfer between enzymes in real biological systems [1]. It can also establish a foundation for fabricating the third-generation biosensors without using redox mediators [2,3]. To obtain and improve direct electrochemistry of redox enzymes, it was proved to be an effective way to incorporate them into various films modified on electrode surface [4,5]. In recent years, for example, our group has studied the direct electrochemistry of redox proteins incorporated in cast films of insoluble surfactants [6], hydrogel polymers [7–9], polyelectrolyte-surfactant [10–12] or clay-surfactant [13] composites, and clay nanoparticles [14]. The proteins or enzymes studied are all heme proteins including myoglobin (Mb), hemoglobin (Hb), and horseradish peroxidase (HRP). All these films greatly enhanced the direct

*Corresponding author. Tel.: +86-106-220-7838; fax: +86-106-220-0567.

E-mail address: hunaifei@bnu.edu.cn (N. Hu).

0301-4622/03/$ - see front matter © 2003 Elsevier Science B.V. All rights reserved.
doi:10.1016/S0301-4622(03)00121-2

electron transfer between the proteins and electrodes compared to that on bare electrodes with the proteins in solution.

Catalase (Cat) (EC 1.11.1.6) is also a heme enzyme, which is present in almost all-aerobic organism [15]. Catalase has a molecular weight of approximately 240 000, and is composed of four identical subunits, each containing a single heme prosthetic group. The heme group consists of a protoporphyrin ring and a central Fe atom, where iron usually is in the ferric oxidation state as its stable resting state [16]. As a catalyst, catalase functions either in the catabolism of H_2O_2 or in the peroxidatic oxidation of small molecule substrates by H_2O_2 [17,18]. Under normal physiological conditions, catalase controls the H_2O_2 concentration so that it does not reach toxic levels that could bring about oxidative damage in cells. The mechanism of disproportionation of H_2O_2 catalyzed by catalase can be expressed as [17,18]:

$$H_2O_2 + \text{CatFe(III)} \rightarrow \text{Compound I} + H_2O \quad (1)$$

$$H_2O_2 + \text{Compound I} \rightarrow \text{CatFe(III)} + O_2 + H_2O \quad (2)$$

where CatFe(III) is the resting state of catalase, Compound I is a two-equivalent oxidized form of CatFe(III) containing an oxyferryl heme ($Fe^{IV}=O$) and a porphyrin π cation radical. H_2O_2 first oxidizes CatFe(III) to form Compound I and H_2O, and then reduces Compound I to CatFe(III) and produces O_2. As a well-known efficient catalyst, catalase acts either as a reductant or as an oxidant in the reactions, and returns to its resting state after one catalytic cycle, while H_2O_2 undergoes dismutation to produce H_2O and O_2.

Although the heme groups are the electroactive center of catalase, it is usually difficult to observe the direct electron exchange of catalase in solution with electrodes, probably because the hemes are buried deeply inside the polypeptide chains of relatively large catalase molecules. Films modified on solid electrodes may provide a new approach to realize its direct electrochemistry. A recent report by Kong et al. [19] showed that in didodecyldimethylammonium bromide (DDAB) films cast on pyrolytic graphite (PG) electrodes, catalase gave a pair of direct cyclic voltammetry (CV) peaks in blank buffers. Rusling and coworkers [20] used dimyristoylphosphatidylcholine (DMPC) as a film-forming material to incorporate catalase. The Cat-DMPC films cast on PG electrodes showed a pair of well-defined, quasi-reversible CV peaks, characteristic of heme Fe(III)/Fe(II) redox couples of catalase. Both DDAB and DMPC are water-insoluble, double-chain surfactants, and can form multibilayer films from their organic solution or aqueous dispersion. It is these biomembrane-like surfactant films that provided a suitable microenvironment for catalase to transfer electron with PG electrodes.

Polyacrylamide (PAM) is a kind of non-ionic polymer. PAM can absorb large amounts of water and form hydrogel, which is widely used in the field of life science. PAM has a long hydrophobic hydrocarbon backbone with one hydrophilic amide group in each of its repeated monomer unit. Such amphiphilic polymers can also be considered as polymeric surfactants. In our previous works, Hb-PAM [21], Mb-PAM [22], and HRP-PAM [23] films modified on PG electrodes demonstrated stable and well-defined CV responses for the heme Fe(III)/Fe(II) couple. Thus, we expect that the PAM hydrogel films could also provide a favorable microenvironment for incorporated catalase, and catalase in PAM films would give a direct electrochemical response at electrodes.

In this paper, Cat-PAM films were cast on PG electrodes and the direct voltammetry of catalase in PAM films were realized and investigated. The Cat-PAM film electrodes also showed good catalytic character toward oxygen and hydrogen peroxide. The mechanism of electrocatalytic reduction of H_2O_2 at Cat-PAM film electrodes was discussed.

2. Experimental

2.1. Chemicals

Beef liver catalase (15 000 units mg^{-1}) was from Sigma and used as received without further purification. Polyacrylamide (MW 3 000 000) was from Shanghai Reagent Company. Hydrogen peroxide (H_2O_2, 30%) was from Beijing Chemical Plant. The buffer was usually 0.05 M potassium

dihydrogen phosphate at pH 7.0 containing 0.1 M KBr. Other supporting electrolytes were 0.1 M sodium acetate, 0.05 M boric acid, or 0.05 M citric acid, all containing 0.1 M KBr. The pHs were regulated with HCl or KOH solutions. Other chemicals were reagent grade. Solutions were prepared using deionized water, which was purified twice successively by ion exchange and distillation.

2.2. Film assembly

Prior to use, basal plane pyrolytic graphite (Advanced Ceramics, geometric area 0.16 cm^2) disk electrodes were polished with metallographic sandpapers of 1200 grit while flushing with water. Electrodes were then ultrasonicated in pure water for 30 s.

To obtain the best CV responses of Cat-PAM films, the experimental conditions for film casting, such as the concentration of catalase, the volume ratio of Cat/PAM, and the total volume of Cat-PAM solution, were optimized. Typically, 10 μl of aqueous solutions containing 6.7 mg ml^{-1} catalase and 0.5 mg ml^{-1} PAM were cast onto a freshly polished PG electrode. A small tube was fit tightly over the electrode to serve as a closed chamber so that the water was evaporated slowly. The Cat-PAM films were then dried in the chamber overnight.

2.3. Apparatus and procedures

A CHI 660 electrochemical workstation (CH Instruments) was used for cyclic voltammetry (CV) and square-wave voltammetry (SWV). A conventional three-electrode cell was used with a saturated calomel electrode (SCE) as reference electrode, a platinum wire as counter electrode, and a PG disk with films as working electrode. Voltammetry on electrodes coated with Cat-PAM films was done in buffers containing no catalase. Buffers were purged with highly purified nitrogen for approximately 15 min before a series of experiments. A nitrogen environment was then kept over solutions in the cell during the experiment. In the experiment with oxygen, measured volumes of pure oxygen were injected through solutions by a syringe in a sealed cell that had been previously degassed with N_2. All experiments were done at ambient temperature of 18 ± 2 °C.

UV–Vis absorption spectroscopy was done with a Cintra 10e UV–visible spectrophotometer (GBC). Sample films for spectroscopy were cast on optical transparent glass slides. Prior to use, the slides were pretreated by ultrasonication in a washing solution (1% KOH + 49% ethanol + 50% water) for 15 min, and then carefully rinsed with water. Cat-PAM films were prepared by depositing Cat-PAM solutions onto the dry slides and then being dried overnight.

Scanning electron microscopy (SEM) was done with an X-650 scanning electron microanalyzer (Hitachi) at an acceleration voltage of 20 kV. Sample films were prepared on PG disks with the same way as for voltammetry. The samples were fixed on the SEM mounting stage with conductive two-sided adhesive tapes. Prior to SEM analysis, approximately 10 nm of Au was coated onto samples with an IB-3 ion coater (Eiko).

3. Results

3.1. Cyclic voltammetry

When a Cat-PAM film electrode was immersed into a pH 7.0 buffer containing no catalase, a pair of well-defined and nearly reversible CV peaks at approximately −0.46 V vs. SCE was observed (Fig. 1b), characteristic of catalase heme Fe(III)/Fe(II) redox couples [19,20]. In contrast, a blank PAM film modified PG electrode in pH 7.0 buffers gave no CV response in the same potential range (Fig. 1a). These results present evidence that the electron transfer between catalase and PG electrodes was greatly enhanced in PAM films. The PAM films provided a suitable microenvironment for catalase to exchange electron with underlying PG electrodes, similar to the systems of Hb-, Mb-, and HRP-PAM [21–23], films. However, the stability of Cat-PAM films was not as good as that of other heme protein-PAM films. While the reduction peak current of Cat-PAM films essentially remained unchanged during the first hour of storage in buffers, the long-term stability experiments showed a 76% decrease of the peak compared

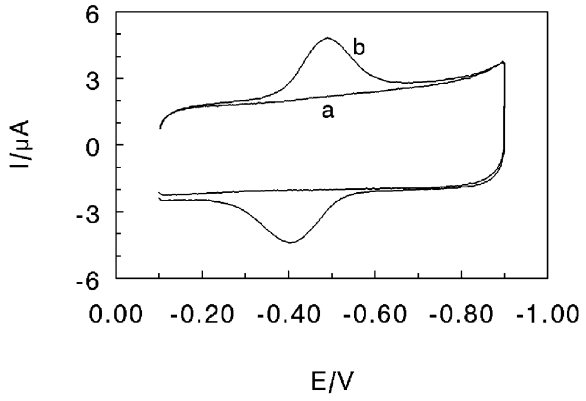

Fig. 1. Cyclic voltammograms at scan rate of 0.2 V s^{-1} in pH 7.0 buffers for (a) PAM film and (b) Cat-PAM film.

with the initial peak height after the films were soaked in the buffer for 8 h. The following voltammetric experiments with Cat-PAM films were thus performed and finished within 1 h.

CVs of Cat-PAM films had approximately symmetric peak shapes and nearly equal heights of reduction and oxidation peaks. Reduction peak current increased linearly with scan rate from 0.1 to 1.0 V s^{-1}. Integration of reduction peaks at different scan rates gave nearly constant charge (Q) values. All these suggest quasi-reversible, diffusionless, surface-confined electrochemical behavior [24], in which all electroactive CatFe(III) in the film is converted to CatFe(II) on the forward cathodic scan, with full conversion of CatFe(II) back to CatFe(III) on the reverse anodic scan. According to the Γ^*–Q relationship [25], the average surface concentration of electroactive catalase (Γ^*) was estimated to be $(2.36 \pm 0.04) \times 10^{-11}$ mol cm^{-2}, which accounted for approximately 1.3% of the total amount of catalase deposited on the electrode surface. This indicates that most catalase molecules in PAM films are not electroactive. Only those in the inner layers of the films closest to the electrode surface and with a suitable orientation are electrochemically addressable and contribute to the observed redox reaction, as in the case of other protein films [9,14].

To examine the possibility of catalase entering PAM films from its solution, a plain PAM film electrode was immerged into a pH 7.0 buffer containing 56 μM catalase, and CVs were run periodically. Both reduction and oxidation peaks centered at approximately −0.46 V grew rapidly with soaking time for the first half an hour, then settled down to a slow increase, suggesting that increasing amounts of catalase entered the PAM films. After approximately 24 h of soaking, the reduction peak current did not increase any more, indicating the PAM films were fully loaded with catalase and the equilibrium of absorption/desorption was reached. This also suggests that there is some kind of interaction between catalase and PAM. Compared with the cast Cat-PAM films, the PAM films fully loaded with catalase showed almost the same CV peak positions and a little larger peak currents. However, the cast method is more convenient and quantitative than the loading method for preparing Cat-PAM films. Thus, in the subsequent experiments, all Cat-PAM films were prepared by the cast mode.

The pH of external solution had great influence on CV peak potentials of Cat-PAM films. An increase of buffer pH led to a negative shift in potential for both reduction and oxidation CV peaks. The formal potential ($E^{\circ\prime}$), estimated as the midpoint of reduction and oxidation peak potentials, varied linearly with pH from 4.0 to 9.0 with a slope of −56 mV pH^{-1} (Fig. 2). This slope value is reasonably close to the theoretical value of −58 mV pH^{-1} at 18 °C for a reversible electron

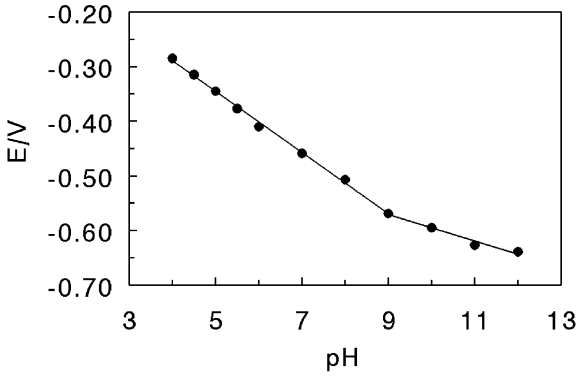

Fig. 2. Influence of pH values on formal potentials for Cat-PAM films at 0.2 V s^{-1}

Table 1
Apparent heterogeneous electron transfer rate constants and formal potentials for various protein films in buffers containing no proteins

Films[a]	pH	Average k_s (s^{-1})	Average $E^{\circ\prime}$ (V vs. SCE)		Reference[b]
			CV	SWV	
Cat-PAM	7.0	29 ± 4	-0.459	-0.481	tw
Cat-CS	7.0	40 ± 7	-0.458	-0.467	[9]
Cat-DDAB	6.1		-0.162		[19]
Cat-DMPC	6.0		-0.426		[20]
Hb-PAM	7.0	45 ± 8	-0.320	-0.312	[21]
Mb-PAM	7.0	86 ± 19	-0.335	-0.357	[22]
HRP-PAM	7.0	72 ± 14	-0.331	-0.321	[23]

[a] PAM = polyacrylamide, CS = chitosan, DDAB = didodecyldimethylammonium bromide, DMPC = dimyristoylphosphatidylcholine.

[b] tw: this work, reporting average values for analysis of eight SWVs at frequencies of 100–161 Hz, amplitudes of 60 and 75 mV, and a step height of 4 mV.

transfer coupled by proton transportation with the equal number of proton and electron [26,27]. Since each catalase molecule has four heme groups, this slope suggests that a single protonation accompanies the one-electron transfer between each heme group and electrodes, represented in general terms by

$$\mathrm{CatFe(III)} + \mathrm{H^+} + \mathrm{e^-} \rightleftharpoons \mathrm{CatFe(II)}$$

An inflection point appeared in the plot at pH 9.0. At pH > 9.0, $E^{\circ\prime}$ varied linearly with pH with a smaller slope. The position of the inflection point in the $E^{\circ\prime}$-pH plot suggests that the protonatable site associated with the electrode reaction has an apparent pK_a value of 9.0.

3.2. Square-wave voltammetry

To estimate the apparent heterogeneous electron transfer rate constant (k_s) and other electrochemical parameters, SWV and non-linear regression methods were used. As discussed in detail previously [28,29], the procedure employed non-linear regression analysis for SWV forward and reverse background-subtracted curves, with the combination of a single-species thin-layer SWV model [30] and a formal potential dispersion model [28,29].

Analysis of SWV data for Cat-PAM films showed goodness of fit onto the 5-$E^{\circ\prime}$ dispersion thin-layer SWV model in the range of various amplitudes and frequencies. The average value of k_s obtained from fitting SWV data at pH 7.0 was 29 s^{-1}, and $E^{\circ\prime}$ was -0.481 V vs. SCE. Parameters for other catalase films and other protein-PAM films are listed in Table 1 for comparison.

For Cat-PAM films, the value of k_s is smaller than that of catalase in chitosan (CS) films and other heme proteins in PAM films, but all of them in the same relative large magnitude. The formal potential of Cat Fe(III)/Fe(II) redox couples in PAM films is close to that of Cat-CS films, but more negative than that of Cat-DDAB and Cat-DMPC films. Different film components may provide different microenvironments for the same protein and influence its formal potential by their interaction with the protein or by their effect on the electrode double-layer [29]. In the same PAM films, catalase showed its formal potential more negative than Mb, Hb, and HRP. This result is in line with that for protein-CS [9] and protein-DMPC films [20]. For instance, in pH 7.0 buffers, Mb-CS films had the formal potential at -0.33 V vs. SCE, while $E^{\circ\prime}$ of Cat-CS films were at -0.46 V, more negative than the former. The reason for this is not clear yet. It may be related with the much larger molecular weight of catalase than the others. Heme inside the larger polypeptide chains of catalase may need more active energy to electrochemically reduce at electrodes. The larger molecule of catalase than other studied heme proteins may also have weaker interaction with PAM films,

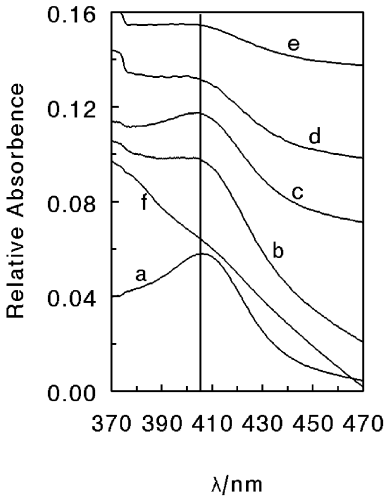

Fig. 3. UV–Vis absorption spectra of (a) dry catalase film, (b) dry Cat-PAM film, and Cat-PAM films in different pH buffer solutions: (c) pH 7.0; (d) pH 5.0; (e) pH 9.0; (f) pH 3.0. The absorbance coordinate only reflects relative absorbance.

which would be probably responsible for the relatively poor stability of catalase in PAM films.

3.3. UV–Vis spectroscopy

The sensitive Soret absorption band of heme proteins may provide information on the protein denaturation, especially on the conformational change of the polypeptides around the heme region [31]. UV–Vis spectroscopy was used to observe the position change of Soret band for Cat-PAM films. Both dry catalase and Cat-PAM films cast on transparent glass slides showed Soret band at 405 nm (Fig. 3a,b), suggesting that catalase in dry PAM films has a secondary structure nearly the same as the native state of catalase in dry catalase films alone. The position of Soret band depended on pH when Cat-PAM films were immersed into buffer solutions. At pH between 5.0 and 9.0, the Soret band appeared at 405 nm (Fig. 3c–e), the same as that of dry Cat-PAM films, indicating that catalase in PAM films essentially retain its native state in buffers at medium pH. When pH was changed toward more acidic or more basic direction, the Soret band showed blue-shift and some distortion. At pH 3.0, for example, even no peak was observed in the studied wavelength range (Fig. 3f), suggesting considerable denaturation of catalase in PAM films at this relatively acidic pH.

3.4. Scanning electron microscopy

SEM was used to observe the surface morphology of both PAM and Cat-PAM films. SEM top views of PAM and Cat-PAM films with the same magnification showed totally different appearance. Top views of a PAM film on PG revealed a bubble-like or needle-like crystal structure (Fig. 4a). SEM top views of PAM films containing catalase, however, appeared relatively featureless (Fig. 4b).

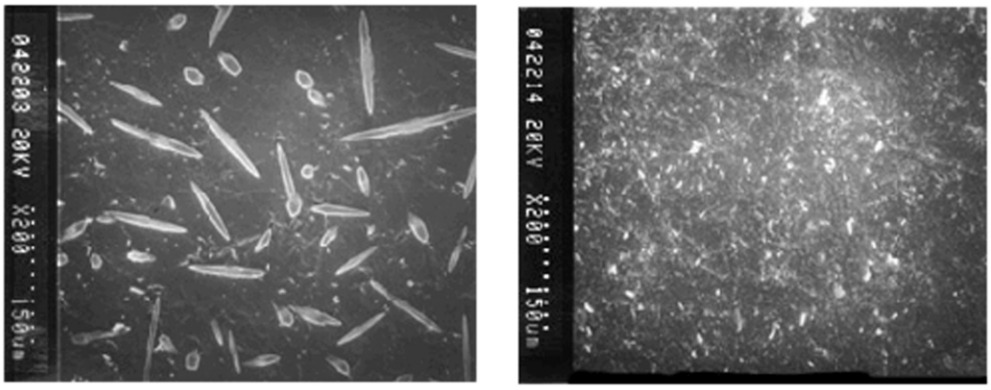

Fig. 4. Top SEM views of coated PG electrodes for (a) PAM film and (b) Cat-PAM film with 200 times magnification.

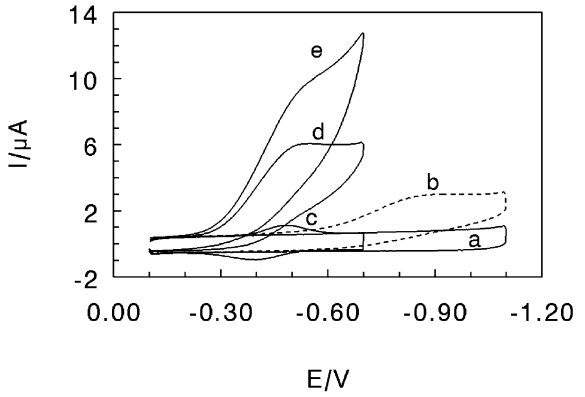

Fig. 5. Cyclic voltammograms at 0.1 V s^{-1} in 10 ml of pH 7.0 buffers for (a) PAM films with no oxygen present, (b) PAM films after 20 ml of oxygen was injected into a sealed cell, (c) Cat-PAM films with no oxygen present, (d) Cat-PAM films after 10 ml of oxygen was injected, and (e) Cat-PAM films after 20 ml of oxygen was injected.

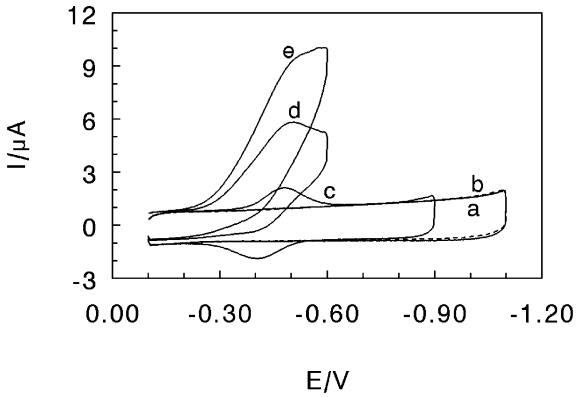

Fig. 6. Cyclic voltammograms at 0.1 V s^{-1} in pH 7.0 buffers for (a) PAM films with no H_2O_2 present, (b) PAM films with 0.8 mM H_2O_2 present, (c) Cat-PAM films with no H_2O_2 present, (d) Cat-PAM films with 0.4 mM H_2O_2 present, and (e) Cat-PAM films with 0.8 mM H_2O_2 present.

SEM picture of Cat-PAM films with larger magnification revealed a structure of closely packed small particles (not shown). All this suggests that interactions between catalase and PAM govern the morphology of the dry films.

3.5. Electrocatalytic reactivity

The electrocatalytic reduction of dioxygen by Cat-PAM films was tested by CV (Fig. 5). When a certain amount of oxygen was passed through a pH 7.0 buffer solution by a syringe, an increase in reduction peak at approximately −0.5 V was observed for Cat-PAM films, accompanied by a disappearance of the oxidation peak for CatFe(II) since CatFe(II) had reacted with oxygen. The reduction peak current increased with the amount of oxygen in solution. For PAM films with no catalase incorporated, the peak for direct reduction of oxygen was observed at approximately −0.85 V. Thus, Cat-PAM films lowered the reduction overpotential of oxygen by approximately 0.35 V.

Reduction of H_2O_2 was also electrochemically catalyzed by Cat-PAM films (Fig. 6). When H_2O_2 was added to a pH 7.0 buffer, an increase in reduction peak at approximately −0.5 V was observed, accompanied by a disappearance of the oxidation peak. An increase in the amount of H_2O_2 in solution increased the reduction peak current. However, direct reduction of H_2O_2 on blank PAM films was not observed in the potential range studied. Catalytic efficiency, expressed as a ratio of reduction peak current of Cat-PAM films in the presence (I_c) and absence (I_d) of H_2O_2, I_c/I_d, decreased with the increase of scan rate (Fig. 7), also characteristic of electrochemical catalysis [32].

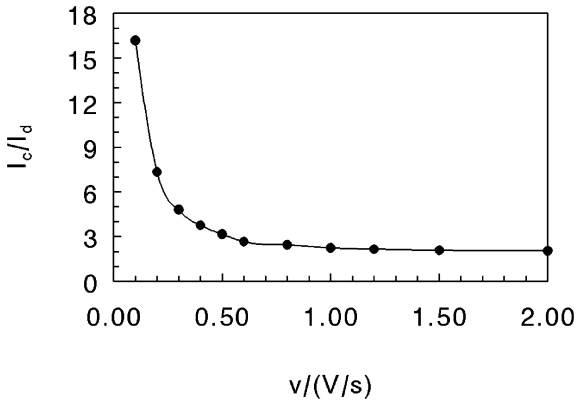

Fig. 7. Influence of scan rates on catalytic efficiency, I_c/I_d, for Cat-PAM film electrode in pH 7.0 buffer with 0.8 mM H_2O_2 present.

4. Discussion

4.1. Effect of PAM films on electrochemistry of catalase

Quasi-reversible CV for catalase was obtained when Cat-PAM films were placed in blank buffer solutions (Fig. 1), suggesting direct electron transfer between catalase and PG electrode in PAM films. Electron transfer was much faster for Cat-PAM films in buffers than for catalase in solution on bare PG, on which electron transfer is so slow as to be difficult to observe. Thus, PAM films must have a great effect on the electron transfer kinetics for catalase and provide a favorable microenvironment for its direct electrochemistry. While the exact nature of this effect is not very clear, the strong hydrophilicity of PAM films and the biocompatibility of polyacrylamide may the main factors. The addition of water to dry PAM films causes an extreme expansion of its volume because of general loosening of the polymer packing density, and the adsorption of large amounts of water results in the formation of polyacrylamide hydrogel [21,22]. This looser structure of polymer in its hydrogel form may provide catalase with a mainly aqueous microenvironment, which is compatible with the biomolecules. Another possibility is that the PAM films inhibit the adsorption of impurities from catalase solutions on the electrodes, which could otherwise block electron transfer for the protein [33]. The large water content of PAM films may also partially explain the ability of PAM films to take up catalase from its solution. The rapid appearance of the redox peaks after the PAM films were immersed in catalase solutions suggests physical diffusion of catalase molecules within the films. The PAM films can be viewed as a hydrogel phase with the high water content, within which some catalase molecules may retain their mobility.

PAM films could take up catalase from its solution at pH 7.0. The CV peak currents grew with soaking time until reaching the steady state in approximately 24 h. However, these results can not be explained by Coulombic attraction between catalase and PAM films. At pH 7.0, with its isoelectric point (p*I*) at pH 5.8 [34], catalase shows negative surface charges, while PAM is essentially neutral on the whole with no charges at this pH. Thus, the driving force for catalase to enter PAM films would be mainly hydrophobic interaction between biomacromolecule catalase and PAM films, in which the long hydrocarbon backbone constitutes the hydrophobic region of the films. This hydrophobic interaction would also be mainly responsible for the retention of catalase in the films in blank buffers. SEM results also imply that PAM films have strong interaction with catalase and it is the interaction that influence the morphology of the protein films.

4.2. Electrocatalytic properties of Cat-PAM films

Cat-PAM films can electrochemically catalyze the reduction of O_2 and H_2O_2, with a significant lowering of overpotential. At Cat-PAM film electrodes, the position of catalytic reduction peak potential of hydrogen peroxide was almost the same as that of oxygen (Figs. 5 and 6), indicating the similarity of the reaction mechanism between the two systems. Catalase is an efficient catalyst for dismutation of hydrogen peroxide, where O_2 and H_2O are the final products [17], and the mechanism is described in Eqs. 1 and 2. It is the production of O_2 that makes the electrocatalytic behavior of H_2O_2 very similar to that of O_2 at Cat-PAM film electrodes. It seems impossible that H_2O_2 would undergo pre-disproportionation in solution when catalase is absent in the films, since no signal was observed at the reduction potential of oxygen at plain PAM film electrodes when H_2O_2 was added to the buffer (Fig. 6b). This indicates that the dismutation of H_2O_2 in the procedure is indeed catalyzed by catalase.

The chemistry of catalase catalysis has not been fully understood yet, but the proposed mechanism of electrocatalytic reduction of dioxygen with Mb in both film and solution phases were discussed in detail previously by Rusling et al. [35,36]. Both Mb and catalase are the heme proteins, in which the same heme prosthetic group is the electroactive center. Thus, a possible mechanism of the electrochemical reactions of hydrogen peroxide catalyzed by Cat-PAM films is postulated as follows:

$$2H_2O_2 \xrightarrow{\text{Cat}} O_2 + 2H_2O \quad (3)$$

$$\mathrm{CatFe(III)} + \mathrm{e^-} + \mathrm{H^+} \rightleftharpoons \mathrm{CatFe(II)} \quad \text{at electrode} \tag{4}$$

$$\mathrm{CatFe(II)} + \mathrm{O_2} \rightarrow \mathrm{CatFe(II)} - \mathrm{O_2} \quad \text{fast} \tag{5}$$

$$\mathrm{CatFe(II)} - \mathrm{O_2} + 2\mathrm{e^-} + 2\mathrm{H^+} \rightarrow \mathrm{CatFe(II)} + \mathrm{H_2O_2} \quad \text{at electrode} \tag{6}$$

There are two catalytic cycles here: CatFe(II) reacts with O_2 and forms CatFe(II)–O_2 in Eq. (5), and produced CatFe(II)–O_2 will receive two electrons at electrodes and return to CatFe(II) again in Eq. (6); H_2O_2 produced in Eq. (6) will participate in Eq. (3) to produce dioxygen which will then induce or promote the catalytic cycle of Eqs. (5) and (6).

5. Conclusions

Catalase incorporated in biocompatible polyacrylamide hydrogel films on pyrolytic graphite electrodes demonstrated direct, nearly reversible cyclic voltammograms. The electron transfer involving the heme Fe(III)/Fe(II) redox couple was much faster than that for catalase in solution on bare PG electrodes. Catalase retained its native states in the PAM films at medium pH. Good electrocatalytic properties of the Cat-PAM films toward oxygen and hydrogen peroxide may have a promising potential in fabricating the third-generation biosensor based on the direct electrochemistry of the enzyme.

Acknowledgments

This work was supported by the National Natural Science Foundation of China (20275006 and 29975003).

References

[1] M.F. Chaplin, C. Bucke, Enzyme Technology, Cambridge University Press, Cambridge, UK, 1990.
[2] L. Gorton, A. Lindgren, T. Larsson, F.D. Munteanu, T. Ruzgas, I. Gazaryan, Direct electron transfer between heme-containing enzymes and electrodes as basis for third generation biosensors, Anal. Chim. Acta 400 (1999) 91–108.
[3] F.A. Armstrong, G.S. Wilson, Recent developments in faradaic bioelectrochemistry, Electrochim. Acta 45 (2000) 2623–2645.
[4] J.F. Rusling, Enzyme bioelectrochemistry in cast biomembrane-like films, Acc. Chem. Res. 31 (1998) 363–369.
[5] N. Hu, Direct Electrochemistry of redox proteins or enzymes at various film electrodes and their possible applications in monitoring some pollutants, Pure Appl. Chem. 73 (2001) 1979–1991.
[6] J. Yang, N. Hu, Direct electron transfer for hemoglobin in biomembrane-like dimyristoyl phosphatidylcholine films on pyrolytic graphite electrodes, Bioelectrochem. Bioenerg. 48 (1999) 117–127.
[7] N. Hu, J.F. Rusling, Electrochemistry and catalysis with myoglobin in hydrated poly(ester sulfonic acid) ionomer films, Langmuir 13 (1997) 4119–4125.
[8] J. Yang, N. Hu, J.F. Rusling, Enhanced electron transfer for hemoglobin in poly(ester sulfonic acid) films on pyrolytic graphite electrodes, J. Electroanal. Chem. 463 (1999) 53–62.
[9] H. Huang, N. Hu, Y. Zeng, G. Zhou, Electrochemistry and electrocatalysis with heme proteins in chitosan biopolymer films, Anal. Biochem. 308 (2002) 141–151.
[10] H. Sun, H. Ma, N. Hu, Electroactive hemoglobin-surfactant-polymer biomembrane-like films, Bioelectrochem. Bioenerg. 49 (1999) 1–10.
[11] Y. Hu, N. Hu, Y. Zeng, Electrochemistry and electrocatalysis with myoglobin in biomembrane-like surfactant-polymer $2C_{12}N^+PA^-$ composite films, Talanta 50 (2000) 1183–1195.
[12] L. Wang, N. Hu, Electrochemistry and electrocatalysis with myoglobin in biomembrane-like DHP-PDDA polyelectrolyte-surfactant complex films, J. Colloid Interface Sci. 236 (2001) 166–172.
[13] X. Chen, N. Hu, Y. Zeng, J.F. Rusling, J. Yang, Ordered electrochemically-active films of hemoglobin, didodecyldimethylammonium ions and clay, Langmuir 15 (1999) 7022–7030.
[14] Y. Zhou, N. Hu, Y. Zeng, J.F. Rusling, Heme protein-clay films: direct electrochemistry and electrochemical catalysis, Langmuir 18 (2002) 211–219.
[15] P. Nicholls, G.R. Schonbaum, in: P.D. Boyer, H. Lardy, K. Myrback (Eds.), The Enzymes, 8, Academic Press, Orlando, 1963, pp. 158–159.
[16] M.R. Murthy, T.J. Reid, A. Sicignano, N. Tanaka, M.G. Rossmann, Structure of beef live catalase, J. Mol. Biol. 152 (1981) 465–499.
[17] D. Voer, J.F. Voet, Biochemistry, 2nd ed, Wiley, New York, 1995.
[18] B. Halliwell, J.M.C. Gutteridge, Free Radicals in Biology and Medicine, 3rd ed, New York, Oxford University Press, 1999, pp. 134–140.
[19] X. Chen, H. Xie, J. Kong, J. Deng, Characterization for didodecyldimethylammonium bromide liquid crystal film entrapping catalase with enhanced direct electron transfer rate, Biosens. Bioelectron. 16 (2001) 115–120.

[20] Z. Zhang, S. Chouchane, R.S. Magliozzo, J.F. Rusling, Direct voltammetry and catalysis with Mycobacterium tuberculosis catalase-peroxidase, peroxidases, and catalase in lipid films, Anal. Chem. 74 (2002) 163–170.
[21] H. Sun, N. Hu, H. Ma, Direct electrochemistry of hemoglobin in polyacrylamide hydrogel films on pyrolytic graphite electrodes, Electroanalysis 12 (2000) 1064–1070.
[22] L. Shen, R. Huang, N. Hu, Myoglobin in polyacrylamide hydrogel films: direct electrochemistry and electrochemical catalysis, Talanta 56 (2002) 1131–1139.
[23] R. Huang, N. Hu, Direct voltammetry and electrochemical catalysis with horseradish peroxidase in polyacrylamide hydrogel films, Biophys. Chem. in press.
[24] R.W. Murray, Chemically modified electrodes, in: A.J. Bard (Ed.), Electroanalytical Chemistry, 13, Marcel Dekker, New York, 1984, pp. 191–368.
[25] A.J. Bard, L.R. Faulkner, Electrochemical Methods, Wiley, New York, 1980.
[26] L. Meites, Polarographic Techniques, 2nd edition, Wiley, New York, 1965.
[27] A.M. Bond, Modern Polarographic Methods in Analytical Chemistry, Marcel Dekker, New York, 1980, pp. 27–45.
[28] Z. Zhang, J.F. Rusling, Elctron transfer between myoglobin and electrodes in thin films of phosphatidylcholines and dehexadecylphosphate, Biophys. Chem. 63 (1997) 133–146.
[29] A.-E.F. Nassar, Z. Zhang, N. Hu, J.F. Rusling, T.F. Kumosinski, Proton-coupled electron transfer from electrodes to myoglobin in ordered biomembrane-like films, J. Phys. Chem. 101 (1997) 2224–2231.
[30] J.J. O'Dea, J.G. Osteryoung, Characterization of quasi-reversible surface processes by square-wave voltammetry, Anal. Chem. 65 (1993) 3090–3097.
[31] P. George, G.I.H. Hanania, Spectrophotometric study of ionizations in methemoglobin, Biochem. J. 55 (1953) 236–243.
[32] C. P. Andrieux, C. Blocman, J.-M. Dumas-Bouchiant, F. M'Halla, J.M. Saveant, Homogeneous redox catalysis of electrochemical reactions; Part V, cyclic voltammetry, J. Electroanal. Chem. 113 (1980) 19–40.
[33] A.-E.F. Nassar, W.S. Willis, J.F. Rusling, Electron transfer from electrodes to myoglobin: facilitated in surfactant films and blocked by absorbed biomacromolecules, Anal. Chem. 67 (1995) 2386–2392.
[34] F. Caruso, D. Trau, H. Mohwald, R. Renneberg, Enzyme encapsulation in layer-by-layer engineered polymer multilayer capsules, Langmuir 16 (2000) 1485–1488.
[35] A.C. Onuoha, J.F. Rusling, Electroactive myoglobin-surfactant films in a bicontinuous microemulsion, Langmuir 11 (1995) 3296–3301.
[36] A.C. Onuoha, X. Zu, J.F. Rusling, Electrochemical generation and reactions of ferrylmyoglobins in water and microemulsions, J. Am. Chem. Soc. 119 (1997) 3979–3986.